

Insights into the semiclassical Wigner treatment of bimolecular collisions

L. Bonnet*

CNRS, Univ. Bordeaux, ISM, UMR 5255, 33405, Talence, France

(Dated: November 13, 2018)

The semiclassical Wigner treatment of bimolecular collisions, proposed by Lee and Scully on a partly intuitive basis [J. Chem. Phys. 73, 2238 (1980)], is derived here from first principles. The derivation combines E. J. Heller's ideas [J. Chem. Phys. 62, 1544 (1975); 65, 1289 (1976); 75, 186 (1981)], the backward picture of molecular collisions [L. Bonnet, J. Chem. Phys. 133, 174108 (2010)] and the microreversibility principle.

I. INTRODUCTION

Quantum mechanical (QM) calculations of molecular reaction dynamics [1–11] are generally much heavier than quasi-classical trajectory calculations [12–14], in particular for polyatomic processes [15–18]. Hence, for several decades, intense researches aim at building semiclassical methods taking into account the largest quantum effects while keeping with the classical description of nuclear motions [19–33]. Moreover, developing such methods naturally leads to shed light on the complex frontier between the quantum and classical descriptions of motion. Last but not least, semiclassical approaches may be used as powerful interpretative tools to rationalize the dynamics of molecular processes.

The semiclassical Wigner treatment of bimolecular collisions proposed by Lee and Scully is among them [24]. When applied to the collinear inelastic collision between He and H₂, or He and HBr, which involve strong quantum interferences and/or classically forbidden vibrational transitions, this approach leads to final state populations in very good agreement with exact quantum ones (at least for the lowest vibrational states of the initial diatom), contrary to the quasi-classical trajectory (QCT) method [24]. This is illustrated in Figs. 1 and 2 for He plus H₂ (note that these results are particularly relevant as comparative semiclassical/quantum studies of collinear processes usually provide more stringent tests of the validity of semiclassical approaches than similar studies for realistic three-dimensional collisions). In addition, the treatment of Lee and Scully is particularly simple to apply. Hence, it is potentially interesting to study realistic molecular collisions involving certain quantum effects (other than tunneling through a potential energy barrier).

However, the original derivation of this treatment [24] appears to rest on somewhat arbitrary basis, as shown later below. The goal of the present work is thus to put this treatment on firmer theoretical grounds by deriving it from first principles.

This work is mainly motivated by the recent extension of the semiclassical Wigner treatment of Heller [25, 26] to triatomic (or triatomic-like polyatomic) photodissociations [33]. For the first time, rotational motions were taken into account in the theory, thus making it applicable to realistic fragmentations, and comparison between its predictions and rigorous quantum results in the case of Guo's triatomic-like model of methyl iodide photodissociation [34] showed nearly quantitative agreement. Since the method of Lee and Scully bears strong resemblance with the one of Brown and Heller, we hope to be able in the future to include rotational motions in the former so as to make it applicable to realistic bimolecular processes. The present work is a preliminary step towards this goal.

The inelastic collision is defined in section II. The Lee-Scully method is summarized in section III. Its derivation from first principles is presented in section IV. Section V concludes.

* Email: laurent.bonnet@u-bordeaux1.fr

II. COLLISIONAL SYSTEM

We consider the collinear inelastic collision between atom A and diatom BC(n). The process takes place in the electronic ground state. R is the distance between A and the center-of-mass of BC, and r is the BC bond length. P and p are the momenta conjugate to R and r , respectively. The classical function of Hamilton reads

$$H = \frac{P^2}{2\mu} + \frac{p^2}{2m} + V(R, r). \quad (1)$$

μ is the reduced mass of A with respect to BC and m , the one of BC. $V(R, r)$ is the potential energy of ABC associated with the electronic ground state. In the asymptotic channel, BC is assumed to be a harmonic oscillator of frequency $\omega/2\pi$. Its initial vibrational state, of energy

$$E_n = \hbar\omega(n + 1/2), \quad (2)$$

is denoted $\chi_n(r)$. This state is real and normalized to unity. The total energy available to the separated fragments is denoted E . The initial collision energy is thus $E_c = E - E_n$ and the initial value of P is

$$P_i = -[2\mu E_c]^{1/2}. \quad (3)$$

The Hamiltonian operator is denoted \hat{H} .

The numerical results presented throughout this work were obtained within the framework of the Secret-Johnson model of He+H₂ collision [35]. In this model, the potential energy is approximated by

$$V(R, r) = \frac{1}{2}m\omega^2(r - r_e)^2 + \exp[\alpha(r - r_e - R)]. \quad (4)$$

μ and m were kept at 2/3 and 1, respectively, \hbar at 1, ω at 1, α at 0.3 and E at 10, otherwise stated. The value of the equilibrium bond length r_e can be arbitrarily chosen.

The central quantity of this work, already shown for He+H₂ in Figs. 1 and 2, is the probability $P_{n'n}$ of transition from BC(n) to BC(n').

III. LEE-SCULLY METHOD

Lee and Scully consider a hybrid model where the initial and final states of BC are treated quantum mechanically, while the initial and final translational states as well as the whole dynamics within the interaction region are treated classically. This choice makes sense, in particular to QCT users accustomed to introduce *ad-hoc* corrections in their trajectory calculations, but from a rigorous point of view, it is arbitrary.

These assumptions lead to the following developments. The final vibrational state of BC can be written as

$$\phi_f(r) = \sum_{j=0}^{\infty} a_j \chi_j(r), \quad (5)$$

for the $\chi_j(r)$'s form a complete basis. Hence, $P_{n'n}$ satisfies

$$P_{n'n} = |a_{n'}|^2 = \left| \int dr \chi_{n'}^*(r) \phi_f(r) \right|^2. \quad (6)$$

Now, any quantity $|Q|^2$ defined by

$$|Q|^2 = \left| \int dr \Psi_1^*(r) \Psi_2(r) \right|^2 \quad (7)$$

is also rigorously given by the phase space overlap

$$|Q|^2 = 2\pi\hbar \int dr dp \rho_1(r, p) \rho_2(r, p), \quad (8)$$

where $\rho_l(r, p)$, $l = 1$ or 2 , is the Wigner density defined by

$$\rho_l(r, p) = \frac{1}{\pi\hbar} \int ds e^{2ips/\hbar} \Psi_l^*(r+s) \Psi_l(r-s) \quad (9)$$

[24–26, 31, 33, 36, 37]. A pedestrian demonstration of the strict equivalence between Eq. (7) and Eqs. (8) and (9) is given in Appendix B of ref. [31]. Consequently, $P_{n'n}$ can be rewritten as

$$P_{n'n} = 2\pi\hbar \int dr dp \rho_{n'}^{vib}(r, p) \rho_f(r, p), \quad (10)$$

where $\rho_{n'}^{vib}(r, p)$ and $\rho_f(r, p)$ are the Wigner distributions corresponding to $\chi_{n'}(r)$ and $\phi_f(r)$, respectively.

From the well known analytical expression of $\chi_{n'}(r)$ and Eq. (9), $\rho_{n'}^{vib}(r, p)$ can be shown to satisfy [26]

$$\rho_{n'}^{vib}(r, p) = \frac{(-1)^{n'}}{\pi\hbar} L_{n'}(\xi) \exp(-\xi/2), \quad (11)$$

where $L_{n'}(\xi)$ is the n' th Laguerre polynomial,

$$\xi = \frac{4E_v}{\hbar\omega} \quad (12)$$

and

$$E_v = \frac{p^2}{2m} + \frac{1}{2}m\omega^2(r - r_e)^2. \quad (13)$$

E_v appears to be the BC vibrational energy.

$\rho_f(r, p)$ is estimated as follows. $\phi_f(r)$ is supposed to result from the “propagation” in time of $\chi_n(r)$ from the reagents onto the products. This loose statement leads, however, to a practical method when extended to the Wigner densities $\rho_f(r, p)$ and $\rho_n^{vib}(r, p)$. $\rho_n^{vib}(r, p)$ can indeed be rewritten as

$$\rho_n^{vib}(r, p) = \int dr_i dp_i \rho_n^{vib}(r_i, p_i) \delta(r - r_i) \delta(p - p_i). \quad (14)$$

Propagating $\rho_n^{vib}(r, p)$ in time amounts to move each delta peak $\delta(r - r_i) \delta(p - p_i)$ in the (r, p) plane along the classical path starting from (r_i, p_i) . This path is also specified by $R = R_i$, supposed to be large enough for BC to vibrate freely, and $P = P_i$. Once the trajectories are back to $R = R_i$, where BC has reached its final vibrational state, each delta peak is located at a given point of coordinates (r_f, p_f) , both depending implicitly on (r_i, p_i) . Consequently,

$$\rho_f(r, p) = \int dr_i dp_i \rho_n^{vib}(r_i, p_i) \delta(r - r_f) \delta(p - p_f). \quad (15)$$

Replacing $\rho_f(r, p)$ in Eq. (10) by the right-hand-side (RHS) of the above equation and integrating over r and p finally leads to the Lee-Scully expression

$$P_{n'n} = 2\pi\hbar \int dr_i dp_i \rho_{n'}^{vib}(r_f, p_f) \rho_n^{vib}(r_i, p_i) \quad (16)$$

(see the third identity of Eq. (21) in ref. [24]). The Lee-Scully results presented in Figs. 1 and 2 have been obtained from a simple Monte-Carlo method based on 10^6 trajectories, with r_i and p_i both randomly selected within the range $[-6, 6]$, and R_i taken at 20.

IV. DERIVATION OF THE LEE-SCULLY METHOD FROM FIRST PRINCIPLES

We now derive a formulation which closely parallels the time-dependent quantum description as far as possible.

A. Link between transition amplitudes and time-evolved wave-packet

Only the main lines of the derivation of transition amplitudes in terms of a time-evolved wave-packet are given in this section, for it is a known result [21]. For clarity's sake, however, more details are given in Appendix A.

We consider at time 0 the wave-packet defined by:

$$\Psi_0(R, r) = \frac{1}{(2\pi)^{1/2}} \int dk g(k) e^{-ik(R-R_i)} \chi_n(r) \quad (17)$$

with

$$g(k) = \left[\frac{1}{\pi^{1/2}\epsilon} \right]^{1/2} e^{-\frac{1}{2}[(k-k_i)/\epsilon]^2}. \quad (18)$$

$\Psi_0(R, r)$ is normalized to unity. Here, R_i is sufficiently large for the whole wave-packet to lie within the asymptotic region where $V(R, r)$ does not depend on R and the vibrational and translational motions are uncoupled. k_i has a

given positive value, thus making the wave-packet moving inward for sufficiently small values of t (propagation is performed forward in time, otherwise stated). The spreading of the wave-packet is inversely proportional to ϵ .

Let $\phi_E^n(R, r)$ be the state of inelastic scattering between A and BC at energy E , with unit incoming flux in channel n . In the asymptotic region, $\phi_E^n(R, r)$ can be written as

$$\phi_E^n(R, r) = \left[\frac{\mu}{2\pi\hbar^2 k_n} \right]^{1/2} e^{-ik_n R} \chi_n(r) + \sum_{n'} S_{n'n} \left[\frac{\mu}{2\pi\hbar^2 k_{n'}} \right]^{1/2} e^{ik_{n'} R} \chi_{n'}(r) \quad (19)$$

with

$$k_{n'} = \frac{1}{\hbar} [2\mu(E - E_{n'})]^{1/2}. \quad (20)$$

The $S_{n'n}$'s are transition amplitudes, or S -matrix elements. The projection of $\phi_E^n(R, r)$ on $\Psi_0(R, r)$ is given by

$$C_n(E) = \int dRdr \phi_E^{n*}(R, r) \Psi_0(R, r). \quad (21)$$

The time-evolved wave-packet can then be written as

$$\Psi_t(R, r) = \sum_j \int dE' C_j(E') \phi_{E'}^n(R, r) e^{-iE't/\hbar}. \quad (22)$$

We now consider at an infinite time the projection

$$Q_{n'n} = \lim_{t \rightarrow +\infty} \int dRdr \left[\frac{\mu}{2\pi\hbar^2 k_{n'}} \right]^{1/2} e^{-ik_{n'} R} \chi_{n'}(r) \Psi_t(R, r) \quad (23)$$

of the outgoing free state associated with E and n' onto the time-evolved wave-packet. From Eqs. (19) and (21)-(23), it is shown in Appendix A that

$$g(k_n) e^{ik_n R_i} S_{n'n} + g(-k_n) e^{-ik_n R_i} \delta_{n'n} = \left[\frac{\hbar^2 k_n}{\mu} \right]^{1/2} Q_{n'n} e^{iEt/\hbar}. \quad (24)$$

This is an important expression of the time-dependent approach to semiclassical dynamics derived by Heller in the mid-seventies [21]. Eq. (24) is analogous to Eq. (4.4) in Heller's work. The only difference is that in the present work, $g(k)$ (see Eq. (18)) can be non zero for negative values of k . This implies the Kronecker symbol $\delta_{n'n}$ in Eq. (24), not present in Eq. (4.4) of ref. [21].

B. Expressing the projection $Q_{n'n}$ in terms of Wigner densities

Analogously to what we have seen in section III, any quantity $|Q|^2$ defined by

$$|Q|^2 = \left| \int dRdr \Psi_1^*(R, r) \Psi_2(R, r) \right|^2 \quad (25)$$

can be rewritten as

$$|Q|^2 = (2\pi\hbar)^2 \int dRdrdPdP \rho_1(R, r, P, p) \rho_2(R, r, P, p) \quad (26)$$

where $\rho_l(R, r, P, p)$, $l = 1$ or 2 , is the Wigner density defined by

$$\rho_l(R, r, P, p) = \frac{1}{(\pi\hbar)^2} \int ds_R ds_r e^{2i(Ps_R + ps_r)/\hbar} \Psi_l^*(R + s_R, r + s_r) \Psi_l(R - s_R, r - s_r) \quad (27)$$

[25, 26, 31, 33]. The strict equivalence between Eq. (25) and Eqs. (26) and (27) can be proved by following the reasoning presented in Appendix B of ref. [31] limited, however, to the case of one configuration space coordinate. In the present case of two spatial coordinates, the developments are more tedious, but present no difficulty.

Setting

$$\Psi_1(R, r) = \left[\frac{\mu}{2\pi\hbar^2 k_{n'}} \right]^{1/2} e^{ik_{n'}R} \chi_{n'}(r) \quad (28)$$

and

$$\Psi_2(R, r) = \Psi_t(R, r), \quad (29)$$

we arrive from Eqs. (26) and (27) at

$$|Q_{n'n}|^2 = (2\pi\hbar)^2 \lim_{t \rightarrow +\infty} \int dRdrdPdP \rho_t(R, r, P, p) \rho_{n'}^{tr}(R, P) \rho_{n'}^{vib}(r, p), \quad (30)$$

where $\rho_t(R, r, P, p)$ is related to $\Psi_t(R, r)$ by Eq. (27), the translational Wigner distribution $\rho_{n'}^{tr}(R, P)$ reads

$$\rho_{n'}^{tr}(R, P) = \frac{1}{\pi\hbar} \int ds e^{2iPs/\hbar} \left[\frac{\mu}{2\pi\hbar^2 k_{n'}} \right] e^{-ik_{n'}(R+s)} e^{ik_{n'}(R-s)} \quad (31)$$

and $\rho_{n'}^{vib}(r, p)$ is given by Eqs. (11)-(13)

Using Eq. (A.2), Eq. (31) transforms to

$$\rho_{n'}^{tr}(R, P) = \left[\frac{\mu}{2\pi\hbar^2 k_{n'}} \right] \frac{2}{\hbar} \delta[2(P - \hbar k_{n'})/\hbar] \quad (32)$$

or equivalently,

$$\rho_{n'}^{tr}(R, P) = \frac{1}{2\pi\hbar} \delta \left[\frac{P^2}{2\mu} - \frac{\hbar^2 k_{n'}^2}{2\mu} \right] \Theta(P), \quad (33)$$

Θ being the function of Heaviside. Eq. (32) is indeed readily obtained from Eq. (33) by means of theorem (A.7).

C. Semiclassical approximation of $|Q_{n'n}|^2$

Eq. (30) provides a formally exact quantum expression of $|Q_{n'n}|^2$. We now introduce in the formulation the following classical ingredient: we consider $\rho_\tau(R, r, P, p)$ as a solution of the Liouville equation [38] instead of the Wigner one [25, 36, 37], i.e., we classically propagate it from $\tau = 0$ to $\tau = t$. In the framework of this assumption, we have

$$\rho_t(R, r, P, p) dR dr dP dp = \rho_0(R_0, r_0, P_0, p_0) dR_0 dr_0 dP_0 dp_0. \quad (34)$$

In this identity, (R, r, P, p) should be understood as the dynamical state of ABC reached at time t when starting from the initial state (R_0, r_0, P_0, p_0) at time 0. Eq. (34) expresses the fact that the probability to lie within $dR dr dP dp$ does not depend on t , a property due to the deterministic nature of classical mechanics.

Using Eq. (34), one may rewrite Eq. (30) as

$$|Q_{n'n}|^2 = (2\pi\hbar)^2 \lim_{t \rightarrow +\infty} \int dR_0 dr_0 dP_0 dp_0 \rho_0(R_0, r_0, P_0, p_0) \rho_{n'}^{tr}(R_t, P_t) \rho_{n'}^{vib}(r_t, p_t), \quad (35)$$

where for clarity's sake, (R, r, P, p) in $\rho_{n'}^{tr}(R, P) \rho_{n'}^{vib}(r, p)$ have been denoted (R_t, r_t, P_t, p_t) in order to emphasize that these coordinates determine the dynamical state of ABC at time t .

From Eqs. (17), (18) and (27), one may show after some mathematical steps presenting no particular difficulty that

$$\rho_0(R_0, r_0, P_0, p_0) = \frac{1}{\pi\hbar} e^{-\epsilon^2(R_0 - R_i)^2} e^{-\left(\frac{P_0 + \hbar k_i}{\hbar \epsilon}\right)^2} \rho_n^{vib}(r_0, p_0), \quad (36)$$

with $\rho_n^{vib}(r_0, p_0)$ given by Eqs. (11)-(13).

In fact, $\rho_{n'}^{vib}(r_t, p_t)$ depends on the vibrational energy at t (see Eqs. (11)-(13)). Moreover, this energy is a constant of motion beyond the frontier between the interaction region and the free products, defined by a given value R_f of R . Therefore, $\rho_{n'}^{vib}(r_t, p_t)$ can be replaced by $\rho_{n'}^{vib}(r_f, p_f)$ in Eq. (35), where r_f and p_f are, respectively, the values of r_t and p_t at the previous frontier. For exactly the same reason, P_t can be replaced by P_f in Eq. (35). We thus have

$$|Q_{n'n}|^2 = (2\pi\hbar)^2 \int dR_0 dr_0 dP_0 dp_0 \rho_0(R_0, r_0, P_0, p_0) \rho_{n'}^{tr}(R_f, P_f) \rho_{n'}^{vib}(r_f, p_f). \quad (37)$$

D. Validity condition of the semiclassical approximation

The validity of Eq. (37) is conditioned by the ability of classical mechanics to propagate $\rho_t(R, r, P, p)$ in a realistic way, i.e., such as it stays sufficiently close to the exact time-evolved Wigner density, solution of the Wigner equation

[25, 36, 37], up to the products.

In fact, one may even be more restrictive than that for the following reasons. First, $\rho_{n'}^{tr}(R_f, P_f)$ forces the kinetic energy to be equal to $E - E_{n'}$, as deduced from Eqs. (20) and (33). Second, $\rho_{n'}^{vib}(r_f, p_f)$ turns out to be negligible for states (r_f, p_f) corresponding to vibrational energies larger than $\sim E_{n'} + 2.5$, as illustrated in Fig. 3 for $n' = 2$. Consequently, the product $\rho_{n'}^{tr}(R_f, P_f) \rho_{n'}^{vib}(r_f, p_f)$ in Eq. (37) limits the integration to phase space states belonging to the energy range $[E - E_{n'}, E + 2.5]$. Defining $f(H)$ by 1 for H within the previous range, and 0 for H outside it, Eq. (37) can then be rewritten as

$$|Q_{n'n}|^2 = (2\pi\hbar)^2 \int dR_0 dr_0 dP_0 dp_0 \rho_0(R_0, r_0, P_0, p_0) f(H) \rho_{n'}^{tr}(R_f, P_f) \rho_{n'}^{vib}(r_f, p_f). \quad (38)$$

The validity of Eq. (37) is thus conditioned by the ability of classical mechanics to propagate $\rho_t(R, r, P, p)f(H)$ in a realistic way.

The projection of $\rho_0(R, r, P, p)f(H)$ onto the (R, P) plane is represented by the green cloud in Fig. 4 for $n' = 2$, $\epsilon = 0.05$ and $k_i = k_n$ (see Eq. (20)). The whole density lies beyond $R = R_f = 20$ units, defining the frontier of the interaction region for the Secrest-Johnson potential energy surface (PES) [35] (see Eq. (4)). The projection of the classically propagated density when it bounces against the repulsive wall of the PES is given by the red cloud in the same graphic. At this instant, the compression of the wave-packet is maximum.

Due to the small value of ϵ , the green cloud is very narrow along the P direction, and very broad along the R direction, by virtue of the uncertainty principle. The red cloud extends from -10 to 20 units mainly along the R -axis, which turns out to be the whole interaction region available at the energy $E = 10$.

The projections of $\rho_0(R, r, P, p)$ and $\rho_0(R, r, P, p)f(H)$ are represented in Fig. 5 for $\epsilon = 20$, a much larger value than previously, the remaining parameters being unchanged. The first projection corresponds to the brown cloud while the second corresponds to the two green ones. These clouds are now very broad along the P direction, and very narrow along the R direction, at the opposite of the previous case. As a matter of fact, multiplying $\rho_0(R, r, P, p)$ by $f(H)$ strongly alters it for large values of ϵ .

On the other hand, the same operation has not effect for $\epsilon = 0.05$, i.e., projecting $\rho_0(R, r, P, p)$ onto the (R, P) plane still leads to the green cloud in Fig. 4.

Fig. 6 is analogous to Fig. 4 for $\epsilon = 20$. The left and right red clouds come from the classical propagation of the lower and upper green clouds, respectively.

For n' different from n , the right red cloud will not contribute to $|Q_{n'n}|^2$. This cloud is indeed obtained by classically propagating $\rho_0(R, r, P, p)f(H)\Theta(P)$. Now, the previous density contains the factorized term $\rho_n^{vib}(r, p)$ (see Eq. (36)) which remains unaltered by the outward propagation and is orthogonal to $\rho_{n'}^{vib}(r, p)$. The overlap between these two densities in Eq. (38) is thus zero (note that the classical propagation is exact here, the PES being flat along the R -axis and quadratic along the r -axis, satisfying thereby the conditions for which the Wigner equation reduces to the Liouville one [25, 36, 37]). $|Q_{n'n}|^2$ is thus only due to the left red cloud, which extends from about -9 to -4 units along the R -axis.

The distributions of R obtained from the bouncing distributions are represented in Fig. 7. As anticipated from the shape of the red cloud in Fig. 4 and the inner red cloud in Fig. 6, the spreading of the distribution is comparable to the size of the interaction region for $\epsilon = 0.05$, while it is ~ 6 times smaller than the same region for $\epsilon = 20$. Now, it is well known [21, 25] that the smaller the extension of a wave-packet in the configuration space, the more accurate the classical propagation of its corresponding Wigner density. The basic reason is that in this limit, one may reasonably approximate the PES by a second order development around the wave-packet, which reduces the Wigner equation to the Liouville one [21, 25, 36, 37]. As a consequence, large values of ϵ , which strongly narrow the R -extension of $\rho_t(R, r, P, p)f(H)$ within the interaction region, are expected to make its classical propagation more realistic, and the prediction of $|Q_{n'n}|^2$ more accurate than small values of ϵ .

On the other hand, there is no control of the r -extension of $\rho_t(R, r, P, p)f(H)$ in the present approach. This makes it better suited to collisions where the reagents are prepared in the lowest excited vibrational states, less spreaded

along the r coordinate.

For n' equal to n , Eq. (37) has less chance to be valid in the limit of large ϵ , as the classically propagated density $\rho_t(R, r, P, p)$ cannot take into account the possible interference between the outgoing and incoming parts of the initial wave-packet, corresponding to the upper and lower green clouds in Fig. 6. However, setting

$$P_{n'n} = |S_{n'n}|^2, \quad (39)$$

$|Q_{n'n}|^2$ is found from Eq. (24) to satisfy

$$g(k_n)^2 P_{n'n} + g(-k_n)^2 \delta_{n'n} + I = \left[\frac{\hbar^2 k_n}{\mu} \right] |Q_{n'n}|^2, \quad (40)$$

where I results from the interference between the first and second terms on the left-hand-side of Eq. (24). This interference is of the same nature as the previous one, but expressed in a time-independent framework. Since Eq. (37) cannot deal with it, it makes sense to remove I from Eq. (40), thus assuming that the population $P_{n'n}$ satisfies

$$g(k_n)^2 P_{n'n} + g(-k_n)^2 \delta_{n'n} = \left[\frac{\hbar^2 k_n}{\mu} \right] |Q_{n'n}|^2. \quad (41)$$

An analytical example is considered in Appendix B which supports the previous assumption. Note that when n' is different from n , Eq. (41) is exact.

The main finding of the present analysis is that ϵ in Eq. (36) has to be taken at a large value in order to maximize the accuracy of the semiclassical Wigner method.

E. Backward description of the dynamics

At the boundary of the interaction region, i.e., at $R = R_f$, Eq. (1) becomes

$$H = \frac{P_f^2}{2\mu} + \frac{p_f^2}{2m} + \frac{1}{2}m\omega^2(r_f - r_e)^2. \quad (42)$$

Using Eqs. (20), (33) and (42), Eq. (37) can be rewritten as

$$|Q_{n'n}|^2 = 2\pi\hbar \int dR_0 dr_0 dP_0 dp_0 \rho_0(R_0, r_0, P_0, p_0) \rho_{n'}^{vib}(r_f, p_f) \delta \left[H - \frac{p_f^2}{2m} - \frac{1}{2}m\omega^2(r_f - r_e)^2 - E + E_{n'} \right]. \quad (43)$$

P_f being necessarily positive, the term $\Theta(P_f)$, coming from Eq. (33), is not necessary to specify in the above integral. In refs. [31, 33, 39], the alternative set of coordinates (t, H, r_f, p_f) was used in place of (R_0, r_0, P_0, p_0) . In these new coordinates, the origin of time corresponds to the instant where the system is at R_f . The pair (r_f, p_f) specifies the internal state of BC at time 0 and H forces P_f to take the value

$$P_f = \left[2\mu \left(H - \frac{p_f^2}{2m} - \frac{1}{2}m\omega^2(r_f - r_e)^2 \right) \right]^{1/2} \quad (44)$$

(see Eq. (42)). (R_f, P_f, r_f, p_f) lies along a given trajectory. Now, any point along this trajectory can be reached from the previous point by moving along the trajectory a given period of time $|t|$ either forward ($t > 0$) or backward ($t < 0$). In other words, given $R_f, (H, r_f, p_f)$ imposes the classical path, and t the location along it. Consequently, (t, H, r_f, p_f) allows to span the whole phase space.

In addition to that, one may show the important property [31, 39–42]

$$dR_0 dr_0 dP_0 dp_0 = dt dH dr_f dp_f \quad (45)$$

(see, in particular, Appendix C of ref. [31]). From Eqs. (43) and (45) and the straightforward integration with respect to H , we finally arrive at

$$|Q_{n'n}|^2 = 2\pi\hbar \int dr_f dp_f \rho_{n'}^{vib}(r_f, p_f) \int_{-\infty}^{+\infty} dt \rho_0(R_t, r_t, P_t, p_t), \quad (46)$$

not forgetting that the delta term in Eq. (33) imposes the condition

$$P_f = \hbar k_{n'}. \quad (47)$$

Finally, (R_t, r_t, P_t, p_t) in Eq. (46) is the value of (R, r, P, p) at time t when starting from (R_f, r_f, P_f, p_f) at time 0 (the meaning of (R_t, r_t, P_t, p_t) is thus different here and in section IV C).

To summarize, the internal state (r_f, p_f) of BC is randomly chosen within appropriate boundaries. Together with Eq. (47), they allow to generate a trajectory from R_f at time 0. The trajectory is then propagated backward in time, i.e., in the direction of the reagent molecule, and $\rho_0(R_t, r_t, P_t, p_t)$ is time-integrated until the trajectory gets back to the separated fragments and $\rho_0(R_t, r_t, P_t, p_t)$ is found to be negligible (in principle, one should also propagate forward in time. This is useless, however, as $\rho_0(R_t, r_t, P_t, p_t)$ is zero for positive values of t). The result is multiplied by the statistical weight $\rho_{n'}^{vib}(r_f, p_f)$ in order to get the integrand of Eq. (46).

Eq. (46) is, however, not in its final form. It can indeed be analytically simplified by integrating over t as follows. $\rho_0(R_t, r_t, P_t, p_t)$ is given by Eq. (36) where we assume that ϵ has a large value so as to maximize the accuracy of $|Q_{n'n}|^2$, as seen in the previous section. $\rho_0(R, r, P, p)$ is thus narrow along the R -axis, stretched along the P -axis, and extends along the latter in the upper and lower half planes, as illustrated in Figs. 5 and 6. Along the trajectory defined by $(R_f, r_f, P_f = \hbar k_{n'}, p_f)$, we have

$$R_t = R_f + \frac{P_f}{\mu} t \quad (48)$$

within the phase space region corresponding to the free fragments with P positive (after the collision). Moreover,

$$R_t = R_i + \frac{P_i}{\mu} [t - t(r_f, p_f)] \quad (49)$$

within the phase space region corresponding to the free fragments with P negative (before the collision). Both P_i and $t(r_f, p_f)$ depend on the “initial conditions” (r_f, p_f) within the backward picture of the dynamics. Note that P_i has a

negative value, since it corresponds to A approaching from BC.

From the previous considerations, the fact that $\rho_0(R, r, P, p)$ lies in the phase space part associated with the free fragments, and Eq. (36), we have

$$\int_{-\infty}^{+\infty} dt \rho_0(R_t, r_t, P_t, p_t) = Q_{in} + Q_{out} \quad (50)$$

with

$$Q_{in} = \frac{1}{\pi\hbar} \rho_n^{vib}(r_i, p_i) e^{-\left(\frac{P_i + \hbar k_i}{\hbar\epsilon}\right)^2} \int_{-\infty}^{+\infty} dt e^{-\epsilon^2 \left(\frac{P_i}{\mu} [t - t(r_f, p_f)]\right)^2} \quad (51)$$

and

$$Q_{out} = \frac{1}{\pi\hbar} \rho_n^{vib}(r_f, p_f) e^{-\left(\frac{P_f + \hbar k_i}{\hbar\epsilon}\right)^2} \int_{-\infty}^{+\infty} dt e^{-\epsilon^2 \left(R_f - R_i + \frac{P_f}{\mu} t\right)^2}. \quad (52)$$

Note that, *stricto sensu*, the upper time limit in Q_{in} and the lower time limit in Q_{out} cannot be $+\infty$ and $-\infty$, respectively. They should be intermediates times, the former being lower than the latter. However, the region where $\rho_0(R, r, P, p)$ takes significant values is expected to be crossed very quickly in both directions, justifying the passage to infinity. Also, since $\rho_n^{vib}(r_t, p_t)$ does only depend on the vibrational energy corresponding to (r_t, p_t) , and this energy is a constant of motion in the asymptotic channel, r_t and p_t have been replaced in Q_{in} by r_i and p_i , their values at time t where $R_t = R_i$. Moreover, they have been replaced in Q_{out} by r_f and p_f .

Using the fact that

$$\int_{-\infty}^{+\infty} dx \frac{e^{-(x/\epsilon)^2}}{\pi^{1/2}\epsilon} = 1 \quad (53)$$

in order to analytically integrate Q_{in} and Q_{out} , and using Eqs. (18), (41) and (50), we arrive at

$$P_{n'n} = 2\pi\hbar \int dr_f dp_f \rho_{n'}^{vib}(r_f, p_f) \rho_n^{vib}(r_i, p_i) U(P_i) \quad (54)$$

with

$$U(P_i) = \frac{\hbar k_n}{|P_i|} \exp \left[\left(\frac{\hbar k_n - \hbar k_i}{\hbar\epsilon} \right)^2 - \left(\frac{P_i + \hbar k_i}{\hbar\epsilon} \right)^2 \right]. \quad (55)$$

In addition, keeping ϵ at a large value so as to maximize the accuracy of the method clearly reduces $U(P_i)$ to $\hbar k_n/|P_i|$. We finally obtain the first key expression of this work:

$$P_{n'n} = 2\pi\hbar \int dr_f dp_f \rho_{n'}^{vib}(r_f, p_f) \rho_n^{vib}(r_i, p_i) \frac{\hbar k_n}{|P_i|}. \quad (56)$$

In the case of the Secret-Johnson model of He+H₂ collinear collision [35], Eq. (56) leads to the blue curves in Fig. 8 (Backward-SCW results). A simple Monte-Carlo approach based on 10^5 trajectories for each value of n' has been used. The agreement with the QM results is very satisfying. The norm, i.e., the sum of final state populations,

appears to be very close to 1 for both $n = 0$ and $n = 1$.

F. Use of microreversibility to reconnect with the standard forward description

Eq. (56) is actually not the expression most suitable for numerical applications. In order to get $P_{n'n}$, one has to run a batch a trajectories backward in time from R_f with P_f given by Eq. (47). If n' runs from 0 to n'_{max} , $n'_{max} + 1$ batches of trajectories must be run in order to obtain the whole final state distribution.

However, the microreversibility principle tells us that, within the framework of quantum mechanics, $P_{n'n} = P_{nn'}$. Hence, if the semiclassical Wigner treatment is realistic, one may rewrite $P_{n'n}$ as

$$P_{n'n} = 2\pi\hbar \int dr_f dp_f \rho_n^{vib}(r_f, p_f) \rho_{n'}^{vib}(r_i, p_i) \frac{\hbar k_{n'}}{|P_i|}. \quad (57)$$

Eq. (57) is just Eq. (56) with n and n' interchanged. P_f is now given by

$$P_f = \hbar k_n. \quad (58)$$

Last but not least, one may arbitrarily interchange the indices i and f in Eq. (57), i.e., call the initial internal conditions r_i and p_i , keep the radial momentum at the negative value

$$P_i = -\hbar k_n, \quad (59)$$

run from R_f the resulting trajectories forward in time, and call the final conditions r_f , p_f and P_f once the trajectory is back to R_f . The ensemble of trajectories run is exactly the same as the one involved in Eq. (57). The only difference is now that P_f is positive, contrary to P_i in Eq. (57). We finally get the second key expression of this work:

$$P_{n'n} = 2\pi\hbar \int dr_i dp_i \rho_n^{vib}(r_i, p_i) \rho_{n'}^{vib}(r_f, p_f) \frac{\hbar k_{n'}}{P_f}. \quad (60)$$

To sum up, the whole final state populations are determined from only one batch of trajectories run from R_f , with (r_i, p_i) randomly chosen within appropriate boundaries and P_i given by Eq. (59). Moreover, the indices i and f refer to initial and final conditions, respectively, and trajectories are integrated forward in time. We have thus reconnected with the traditional way of simulating a molecular collision.

Eq. (60) leads to the blue curves in Fig. 9 (Forward-SCW results). They have been obtained from 10^6 trajectories, with r_i and p_i both randomly selected within the range $[-6, 6]$. The agreement with the QM results is still very satisfying for $n = 0$, a bit less for $n = 1$ as compared with the Backward method. This illustrates the fact that microreversibility is not strictly satisfied by the semiclassical Wigner method. The norm is again very close to 1 for both $n = 0$ and $n = 1$. One notes that the Forward-SCW results are in excellent agreement with the Lee-Scully ones (see Figs. 1 and 2).

G. Recovering the expression of Lee and Scully

The distribution of the ratio $\hbar k_{n'}/P_f$, weighted by $|\rho_n^{vib}(r_i, p_i)\rho_{n'}^{vib}(r_f, p_f)|$ in order to take into account the values which more contribute to $P_{n'n}$ (see Eq. (60)), is represented in Fig. 10 for $n = 0$ and $n' = 1 - 3$, corresponding to the three largest populations (see the upper panel in Fig. 1). Similar distributions are found for $n = 1$. They appear to be peaked around 1. One may thus approximate $\hbar k_{n'}/P_f$ by 1 in Eq. (60), hence, recovering Eq. (16).

The reason why $\hbar k_{n'}/P_f$ is on average close to 1 in the model of He+H₂ collision considered here is that a large part of the available energy E is channeled into the recoil motion. In the limit where the vibrational energy $E_{n'}$ is negligible as compared to E , Eq. (20) leads to

$$\hbar k_{n'} \approx (2\mu E)^{1/2}. \quad (61)$$

Moreover,

$$H = \frac{\hbar^2 k_n^2}{2\mu} + \frac{p_i^2}{2m} + \frac{1}{2}m\omega^2(r_i - r_e)^2, \quad (62)$$

with k_n given by Eq. (20). Hence, we have from Eqs. (44) and (62)

$$P_f = \left[2\mu \left(E - E_n + \frac{p_i^2}{2m} + \frac{1}{2}m\omega^2(r_i - r_e)^2 - \frac{p_f^2}{2m} - \frac{1}{2}m\omega^2(r_f - r_e)^2 \right) \right]^{1/2}. \quad (63)$$

But if E is much larger than the vibrational energies involved in the problem, we also have

$$P_f \approx (2\mu E)^{1/2}. \quad (64)$$

Since both $\hbar k_{n'}$ and P_f have nearly the same value, their ratio is roughly equal to 1. This explains the shape of the distributions displayed in Fig. 10.

However, this reasoning is no longer valid when $E_{n'}$ may be larger than the recoil energy. In such a case, there is *a priori* no reason for replacing $\hbar k_{n'}/P_f$ by 1 in Eq. (60). The same reasoning holds for $\hbar k_{n'}/|P_i|$ in Eq. (56).

Last but not least, the Forward-SCW and Lee-Scully norms obtained from 5.10^6 trajectories (with r_i and p_i still randomly selected within the range $[-6,6]$) have been calculated. For $n = 0$, the norms obtained by means of Eq. (60)(Eq. (16)) are 0.9984(0.9968), 0.9993(0.9985), 0.9995(0.9984) and 1.0003(0.9995) for $E = 10, 8, 6$ and 3 , respectively. For $n = 1$, the analogous numbers are 0.9952(0.9922), 0.9907(0.9881), 0.9918(0.9862) and 1.0002(0.9980). Moreover, it has been checked that the number a trajectories run is sufficiently large for guarantying the order of the norms between the two approaches. As can be observed, the norm seems to be systematically more underestimated by the Lee-Scully expression than by the Forward-SCW one. Though the differences between the two sets of results are very small, they nevertheless support the idea that the Lee-Scully expression is an approximation to the Forward-SCW expression (though an excellent one). Note that for $n = 2$, the norms are on average equal to ~ 0.94 and the previous order is lost. However, the extension of the initial phase space density along the r coordinate (see Eq. (36)) is larger than for $n = 0$ and 1 , thus making the semiclassical Wigner predictions less reliable.

V. CONCLUSION

About three decades ago, Lee and Scully proposed a semiclassical Wigner treatment of bimolecular collisions [24] leading to final state populations in surprisingly good agreement with exact quantum ones in the case of the Secrest-Johnson model of collinear inelastic collision between He and H₂ [35].

The aim of the present paper was to provide a derivation from first principles of the previous method, following the quantum description as far as possible. The derivation combines elements of (i) the time-dependent approach to semiclassical dynamics [21], (ii) the semiclassical Wigner treatment of photodissociation dynamics [25, 26], the backward description of molecular collisions [31, 39] and (iv) microreversibility.

The Lee-Scully expression of final state populations (Eq. (16)) turns out to be the limiting form of a more general expression (Eq. (60)) when a significant part of the product available energy is channeled into the recoil motion.

The present derivation is focused on collinear inelastic collisions, but defines the main lines of a strategy that could be applicable to realistic three-dimensional bimolecular processes.

Appendix A: Detailed derivation of the link between transition amplitudes and time-evolved wave-packet

1. Projection $C_j(E)$ of $\phi_E^j(R, r)$ on $\Psi_0(R, r)$

From Eqs. (17), (19) and (21) and integration over r , we arrive at

$$C_j(E) = \left[\frac{\mu}{\hbar^2 k_j} \right]^{1/2} \delta_{nj} \int dk g(k) e^{ikR_i} \frac{1}{2\pi} \int dR e^{i(k_j - k)R} + \left[\frac{\mu}{\hbar^2 k_n} \right]^{1/2} S_{nj}^* \int dk g(k) e^{ikR_i} \frac{1}{2\pi} \int dR e^{-i(k_n + k)R}. \quad (\text{A.1})$$

Since

$$\frac{1}{2\pi} \int dR e^{i(k_n - k)R} = \delta(k_n - k), \quad (\text{A.2})$$

we get, by integration over k ,

$$C_j(E) = \left[\frac{\mu}{\hbar^2 k_n} \right]^{1/2} [\delta_{nj} g(k_n) e^{ik_n R_i} + S_{nj}^* g(-k_n) e^{-ik_n R_i}]. \quad (\text{A.3})$$

2. Scattered wave-packet

For t tending to infinity, the time-evolved wave-packet $\Psi_t(R, r)$ (see Eq. (22)) entirely lies in the asymptotic channel and is moving outward. Its overlap with the incoming part of $\phi_{E'}^n(R, r)$ (see Eq. (19)) is thus zero and Eqs. (19) and (22) lead thus to

$$\lim_{t \rightarrow +\infty} \Psi_t(R, r) = \sum_j \int dE' C_j(E') \sum_{n''} S_{n''j} \left[\frac{\mu}{2\pi \hbar^2 k_{n''}} \right]^{1/2} e^{ik_{n''} R} \chi_{n''}(r) e^{-iE't/\hbar}. \quad (\text{A.4})$$

3. Projection $Q_{n'n}$

Replacing in the projection $Q_{n'n}$ (see Eq. (23)) $\Psi_t(R, r)$ by the RHS of Eq. (A.4) and integrating over r leads to

$$Q_{n'n} = \lim_{t \rightarrow +\infty} \sum_j \int dE' \frac{\mu}{\hbar^2} \left[\frac{1}{k_{n'}(E') k_n(E)} \right]^{1/2} C_{j'}(E') S_{n'j}(E') \frac{1}{2\pi} \int dR e^{i[k_{n'}(E') - k_n(E)]R} e^{-iE't/\hbar}. \quad (\text{A.5})$$

For clarity's sake, the dependence of $k_{n'}$ and $S_{n'j}$ on the energy is explicitly specified in the previous expression. Using Eq. (A.2), Eq. (A.5) becomes

$$Q_{n'n} = \lim_{t \rightarrow +\infty} \sum_j \int dE' \frac{\mu}{\hbar^2} \left[\frac{1}{k_{n'}(E') k_n(E)} \right]^{1/2} C_{j'}(E') S_{n'j}(E') \delta[k_{n'}(E') - k_n(E)] e^{-iE't/\hbar}. \quad (\text{A.6})$$

Applying the theorem

$$\delta[f(x)] = \sum_k \frac{1}{|f'(x_k)|} \delta(x - x_k), \quad (\text{A.7})$$

where the x_k 's are solutions of $f(x) = 0$ [43], we find

$$Q_{n'n} = \sum_j C_j(E) S_{n'j} e^{-iEt/\hbar}. \quad (\text{A.8})$$

From Eqs. (A.3) and (A.8), we arrive at

$$Q_{n'n} = \left[\frac{\mu}{\hbar^2 k_n} \right]^{1/2} \left[g(k_n) e^{ik_n R_i} S_{n'n} + g(-k_n) e^{-ik_n R_i} \sum_j S_{nj}^* S_{n'j} \right] e^{-iEt/\hbar}. \quad (\text{A.9})$$

However, $\mathbf{S}^\dagger \mathbf{S} = \mathbf{1}$, where \mathbf{S} is the S -matrix, thus implying

$$\sum_j S_{nj}^* S_{n'j} = \delta_{n'n}. \quad (\text{A.10})$$

From Eqs. (A.9) and (A.10), we finally arrive at Eq. (24).

Analytical example supporting the use of Eq. (41)

In this example, k_i is kept at 0 in Eq. (18), so $g(k) = g(-k)$. Moreover, the potential energy is given by

$$V(R, r) = \frac{1}{2}m\omega^2(r - r_e)^2 \quad (\text{B.1})$$

for $R \geq 0$, and $+\infty$ for $R < 0$. If so, no inelastic transition is possible and we have

$$\phi_E^n(R, r) = \left[\frac{\mu}{2\pi\hbar^2 k_n} \right]^{1/2} \chi_n(r) [e^{-ik_n R} + S_{nn} e^{ik_n R}]. \quad (\text{B.2})$$

Since $\phi_E^n(R, r)$ is 0 for $R = 0$,

$$S_{nn} = -1. \quad (\text{B.3})$$

Squaring both sides of Eq. (24) leads to

$$g(k_n)^2 [P_{nn} + 1 + 2Re(S_{nn} e^{ik_n R_i})] = \left[\frac{\hbar^2 k_n}{\mu} \right] |Q_{nn}|^2. \quad (\text{B.4})$$

This is Eq. (40) for $n' = n$.

Besides, we may apply Eq. (37), together with Eqs. (33) and (36). In a first step, one can replace r_f and p_f in $\rho_n^{vib}(r_f, p_f)$ by r_0 and p_0 , owing to the fact that the vibrational energy E_v is a constant of motion throughout the whole collision, and $\rho_n^{vib}(r_f, p_f)$ does only depend on E_v (see Eqs. (11)-(13)). Since

$$2\pi\hbar \int dr_0 dp_0 \rho_n^{vib}(r_0, p_0)^2 = 1 \quad (\text{B.5})$$

[24], we arrive at

$$|Q_{nn}|^2 = 2 \int dR_0 dP_0 e^{-\epsilon^2(R_0 - R_i)^2} e^{-\left(\frac{P_0}{\hbar c}\right)^2} \rho_n^{tr}(R_f, P_f). \quad (\text{B.6})$$

As the translational motion is unperturbed by the bouncing, P_f in $\rho_n^{tr}(R_f, P_f)$ can be replaced by P_0 . Using Eqs. (33), (A.7) and (18), one gets after integrating over R_0 and P_0 ,

$$|Q_{nn}|^2 = \frac{2\mu g(k_n)^2}{\hbar^2 k_n}. \quad (\text{B.7})$$

Since $P_{nn} = 1$, Eq. (B.7) can be rewritten as

$$g(k_n)^2 (P_{nn} + 1) = \left[\frac{\hbar^2 k_n}{\mu} \right] |Q_{nn}|^2, \quad (\text{B.8})$$

which is just Eq. (41) for $n' = n$. The semiclassical expectation of $|Q_{n'n}|^2$ is thus solution of Eq. (B.4), or Eq. (40), with the interference term removed.

-
- [1] G. Nyman and H.-G. Yu, *Int. Rev. Phys. Chem.* **32**, 39 (2013)
- [2] S. Mahapatra, *Int. Rev. Phys. Chem.* **23**, 483 (2004)
- [3] P. Honvault and J.-M. Launay, *Theory of Chemical Reaction Dynamics* (Kluwer Academic, Dordrecht, The Netherlands, 2004).
- [4] S. C. Althorpe, *Int. Rev. Phys. Chem.* **23**, 219 (2004)
- [5] W. Hu and G. C. Schatz, *J. Chem. Phys.* **125**, 132301 (2006)
- [6] B. Lepetit, D. Wang and A. Kuppermann, *J. Chem. Phys.* **125**, 133505 (2006)
- [7] X. Q. Zhang, Q. Cui, J. Z. H. Zhang and K. L. Han, *J. Chem. Phys.* **126**, 234304 (2007)
- [8] D. De Fazio, J. M. Lucas, V. Aquilanti and S. Cavalli, *Phys. Chem. Chem. Phys.* **13**, 8571 (2011).
- [9] A. Kuppermann, *Phys. Chem. Chem. Phys.* **13**, 8259 (2011).
- [10] C. R. Evenhuis and U. Manthe, *J. Phys. Chem. A* **115**, 5992 (2011)
- [11] S. Liu, X. Xu and D. H. Zhang, *J. Chem. Phys.* **136**, 144302 (2012)
- [12] R. N. Porter and L. M. Raff, in *Dynamics of Molecular Collisions*, edited by W. H. Miller (Plenum, New York, 1976).
- [13] T. D. Sewell and D. L. Thomson, *Int. J. Mod. Phys. B* **11**, 1067 (1997).
- [14] F. J. Aoiz, L. Bañares and V. J. Herrero, *J. Chem. Soc. Faraday Trans.* **94**, 2483 (1998).
- [15] J. Espinosa-García, L. Bonnet, and J.C. Corchado, *Phys. Chem. Chem. Phys.* **12**, 3873 (2010).
- [16] J. D. Sierra, L. Bonnet and M. González, *J. Phys. Chem. A* **115**, 7413 (2011)
- [17] G. Czako, Y. Wang, and J.M. Bowman, *J. Chem. Phys.*, **135**, 151102 (2011).
- [18] G. Czako, *J. Phys. Chem. A*, **116**, 7467 (2012).
- [19] W. H. Miller, *Adv. Chem. Phys.*, **25**, 69 (1974).
- [20] W. H. Miller, *Adv. Chem. Phys.*, **30**, 77 (1975).
- [21] E. J. Heller, *J. Chem. Phys.*, **62**, 1544 (1975).
- [22] J. R. Stine and R. A. Marcus, *Chem. Phys. Lett.*, **29**, 575 (1974).
- [23] J. N. L. Connor, *Chem. Soc. Rev.*, **5**, 125 (1976).
- [24] H.-W. Lee and M. O. Scully, *J. Chem. Phys.*, **73**, 2238 (1980).
- [25] E. J. Heller, *J. Chem. Phys.*, **65**, 1289 (1976).
- [26] R. C. Brown and E. J. Heller, *J. Chem. Phys.*, **75**, 186 (1981).
- [27] M. S. Child, *Semiclassical Mechanics with Molecular Applications*, (Oxford University Press, USA, 1991).
- [28] G. van de Sand and J. M. Rost, *J. Phys. B*, **33**, 1423 (2000).
- [29] Y. Elran and K. G. Kay, *J. Chem. Phys.*, **114**, 4362 (2001).
- [30] J. G. López and A. B. McCoy, *Chem. Phys.*, **308**, 267 (2005).
- [31] L. Bonnet, *Int. Rev. Phys. Chem.*, **32**, 171 (2013).
- [32] L. Bonnet and C. Crespos, *Phys. Rev. A*, **78**, 062713 (2008) ; *ibid*, **80**, 059903(E) (2009).
- [33] W. Arbelo-González, L. Bonnet and A. García-Vela, *Phys. Chem. Chem. Phys.*, **15**, 9994 (2013).
- [34] H. Guo, *J. Chem. Phys.*, **96**, 6629 (1992).
- [35] D. Secrest and B. R. Johnson, *J. Chem. Phys.* **45**, 4556 (1966).
- [36] E. Wigner, *Phys. Rev.*, **40**, 749 (1932).
- [37] H.-W. Lee and M. O. Scully, *Foundations of Physics*, **13**, 61 (1983)
- [38] H. Goldstein, *Classical Mechanics* (Addison-Wesley, MA, 2nd edn, 1980).
- [39] L. Bonnet, *J. Chem. Phys.*, **133**, 174108 (2010)
- [40] M. C. Gutzwiller, *Chaos in Classical and Quantum Mechanics* (Springer, 1990), Chapter 7.5.
- [41] Y. Elran and K. G. Kay, *J. Chem. Phys.* **110**, 8912 (1999).
- [42] K. G. Kay, *J. Chem. Phys.* **132**, 244110 (2010)..
- [43] C. Cohen-Tannoudji, B. Diu and F. Laloë, *Quantum Mechanics* (Hermann, Paris, 1977), see Appendix II.

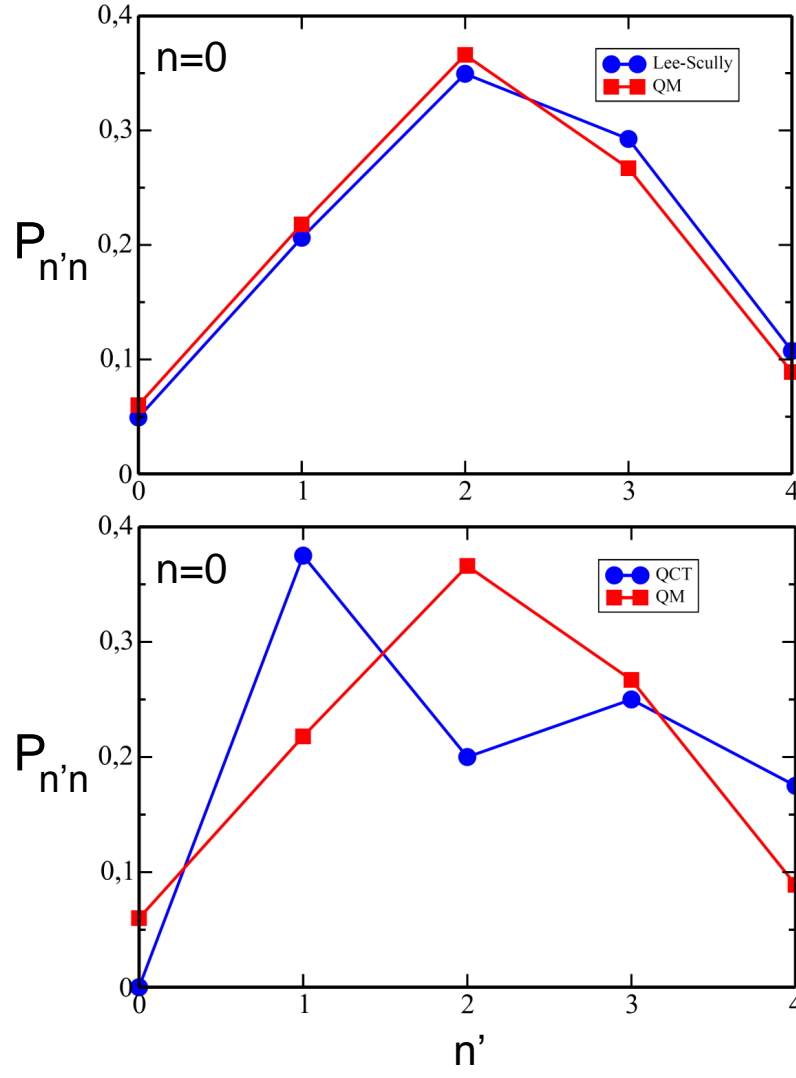


FIG. 1: Final vibrational state distribution for the Secret-Johnson model of collinear collision $\text{He}+\text{H}_2(n) \rightarrow \text{He}+\text{H}_2(n')$ at a total energy of 10 and for $n = 0$. Lee-Scully predictions, given by Eq. (16), and QCT ones are compared with QM results in the upper and lower panels, respectively. QM and QCT data come from refs. [35] and [24], respectively.

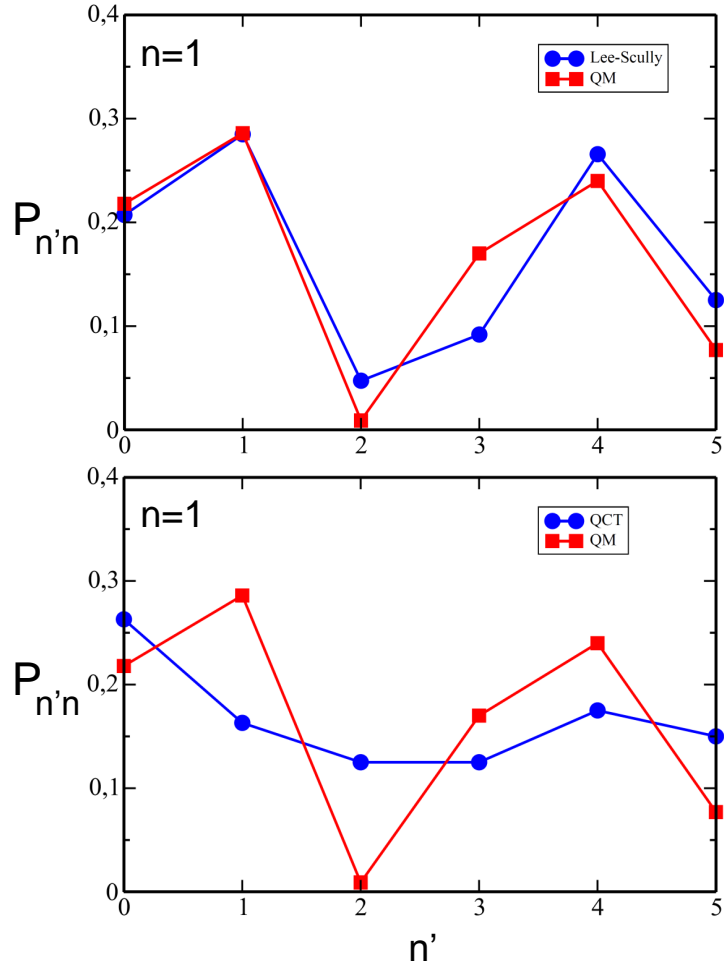


FIG. 2: Same as Fig. 1 for $n = 1$.

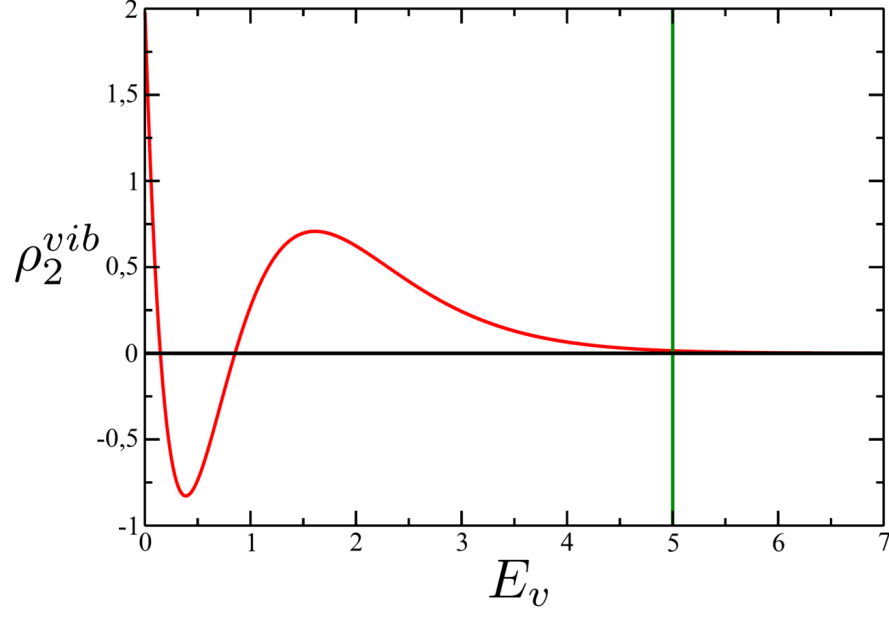


FIG. 3: Wigner distribution ρ_2^{vib} for the harmonic oscillator (see Eqs. (11)-(13)) in terms of the vibrational energy E_v (red curve). On the RHS of the green vertical line, defined by $E_v = E_2 + 2.5 = 5$ (see Eq. (2) with the parameters of section II), ρ_2^{vib} appears to be negligible.

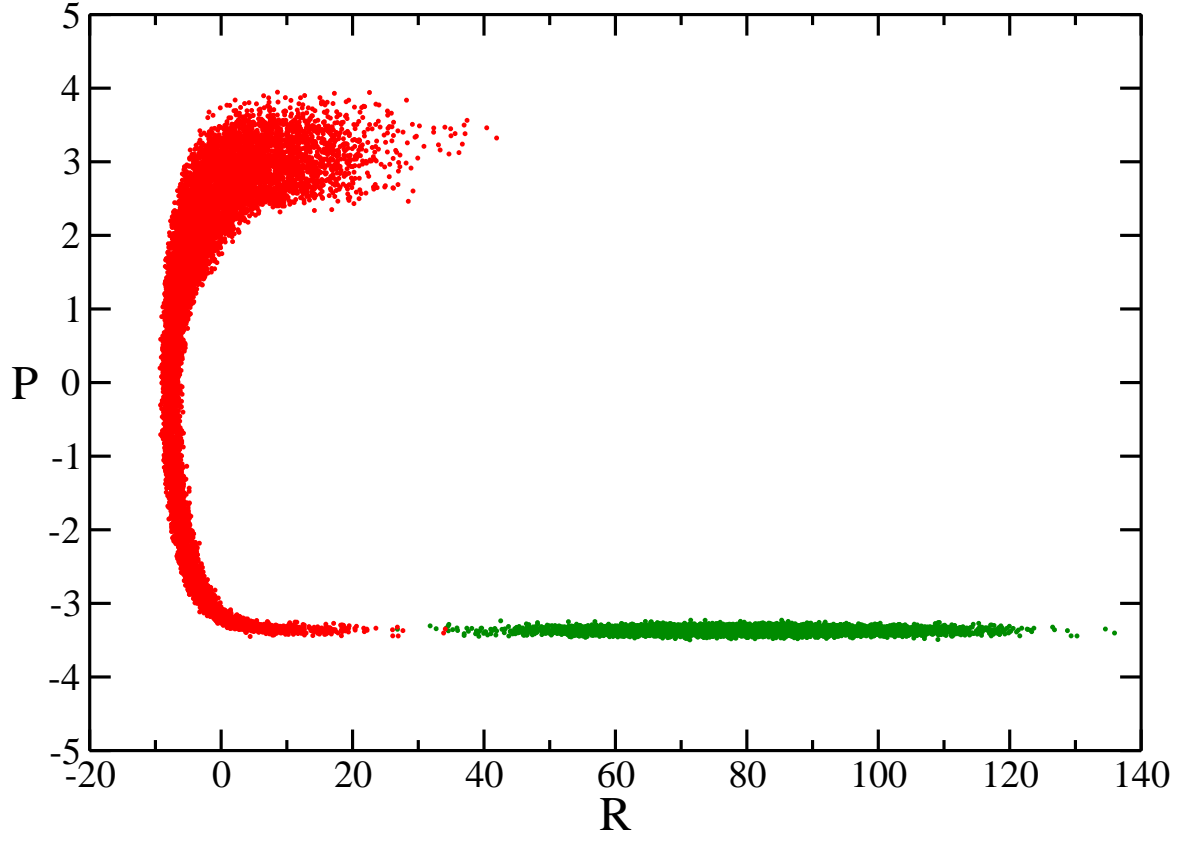


FIG. 4: Green cloud: projection of $\rho_0(R, r, P, p)f(H)$ onto the (R, P) plane for $n' = 2$, $\epsilon = 0.05$ and $k_i = k_n$. Red cloud: projection of the classically propagated previous cloud when it bounces against the repulsive wall of the Secret-Johnson PES.

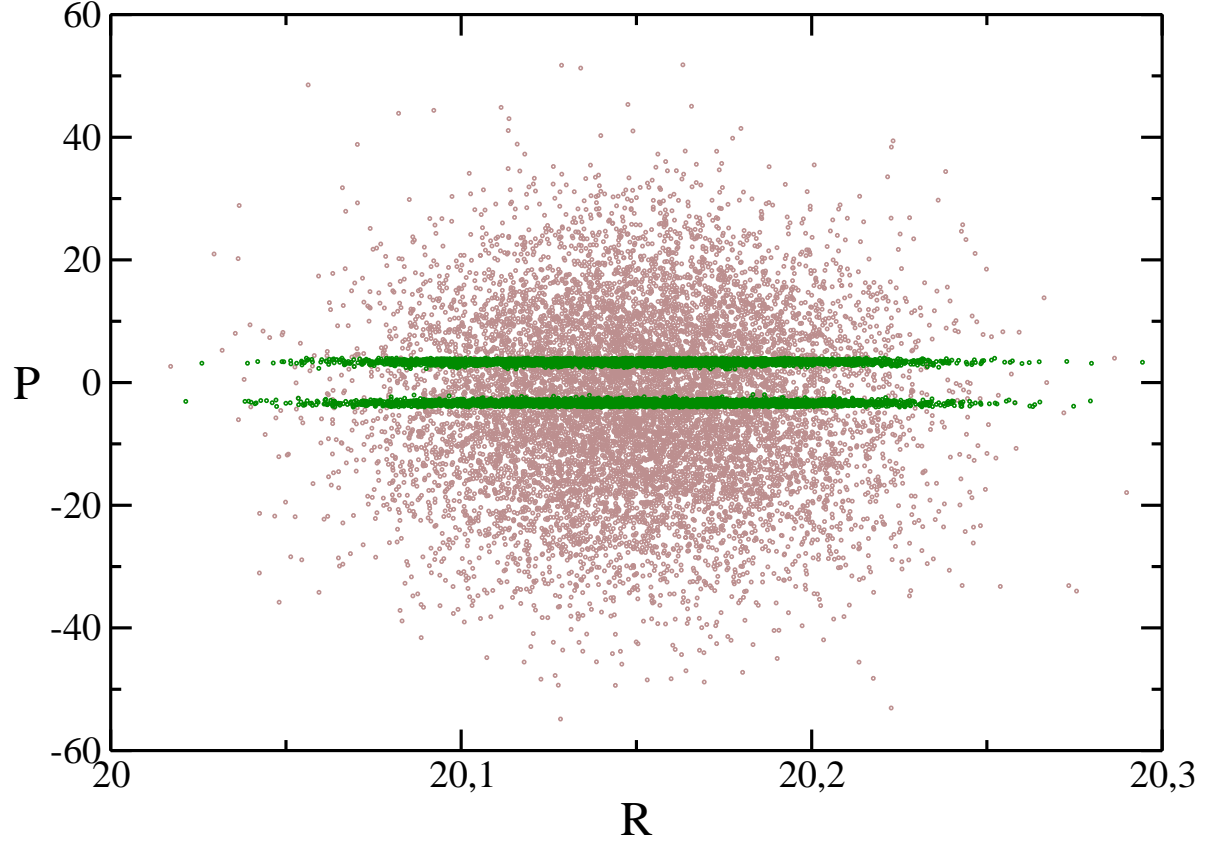


FIG. 5: Brown cloud: projection of $\rho_0(R, r, P, p)$ onto the (R, P) plane for $n' = 2$, $\epsilon = 20$ and $k_i = k_n$. Green cloud: projection of $\rho_0(R, r, P, p)f(H)$ for the same parameters.

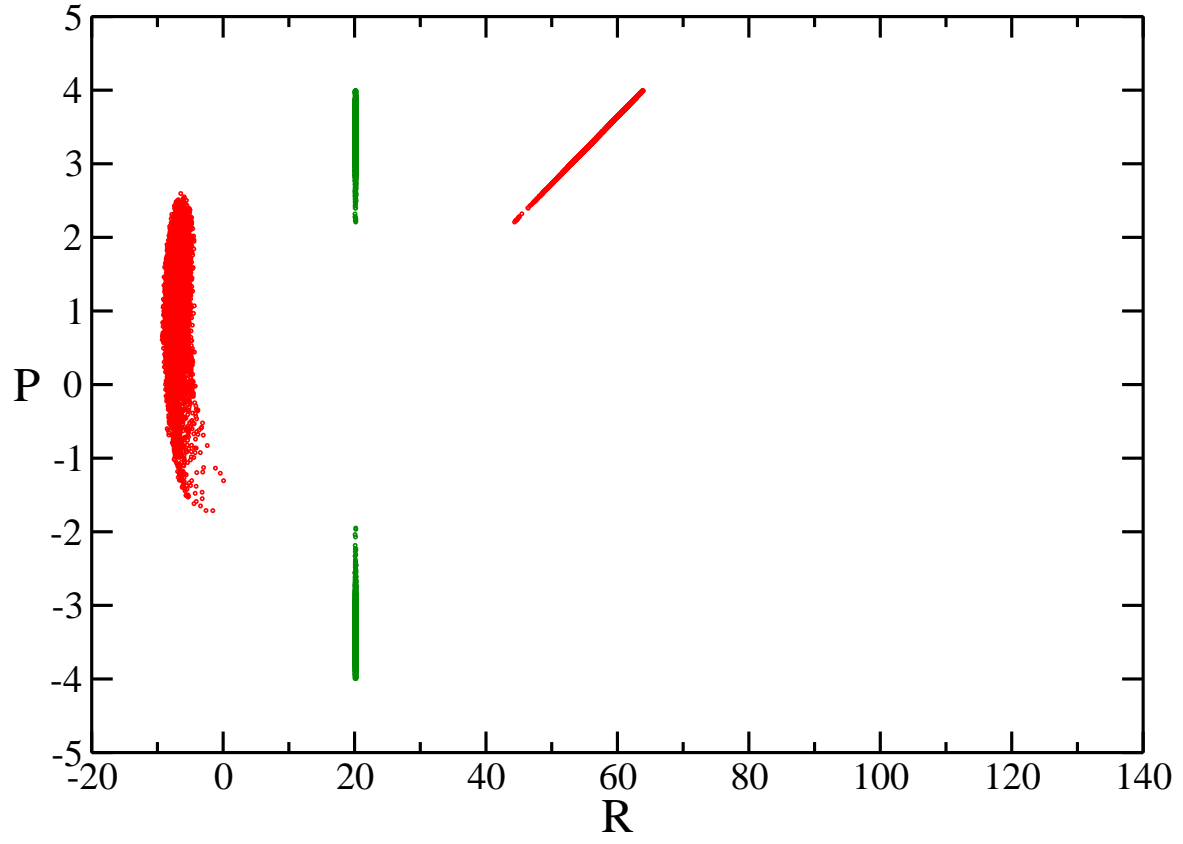


FIG. 6: Same as Fig. 4 for $n' = 2$, $\epsilon = 20$ and $k_i = k_n$.

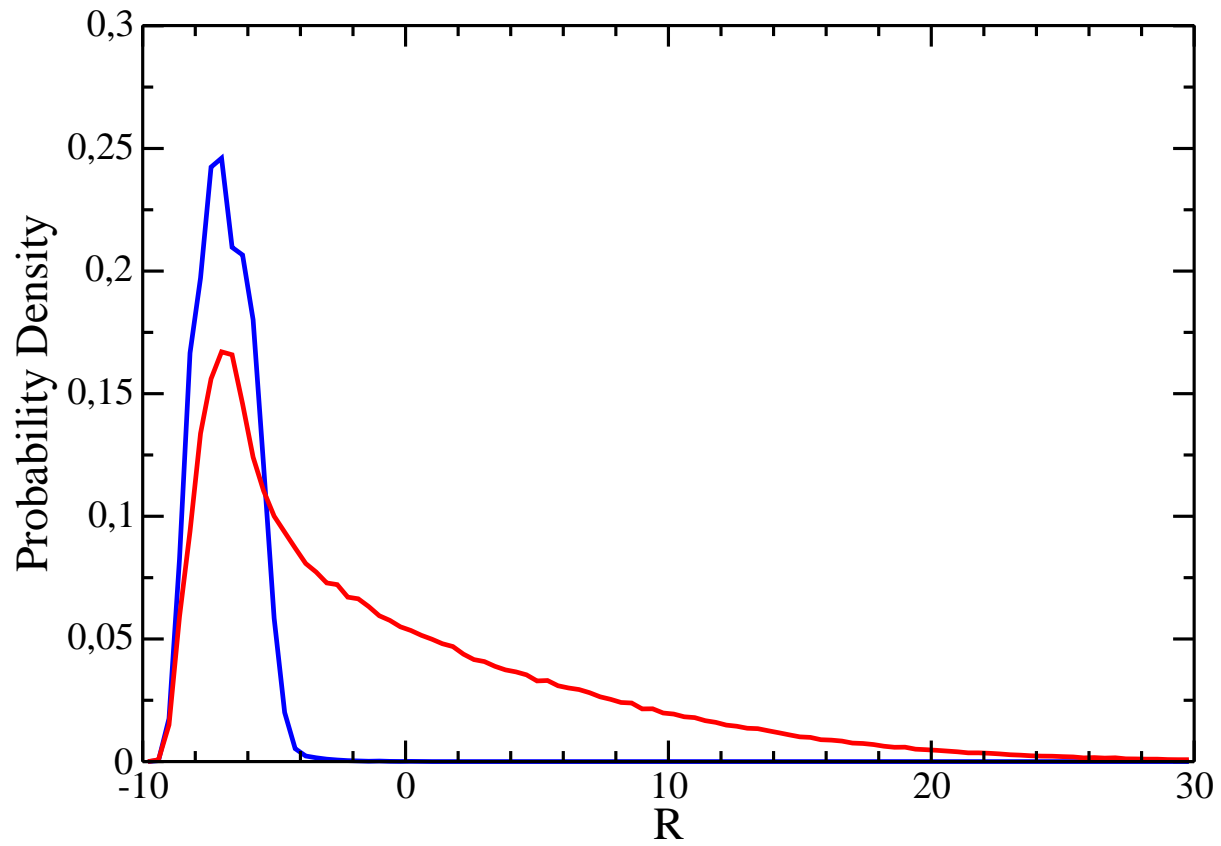


FIG. 7: Distributions of R obtained from the red cloud in Fig. 4 (red curve, corresponding to $\epsilon = 0.05$) and the inner red cloud in Fig. 6 (blue curve corresponding to $\epsilon = 20$).

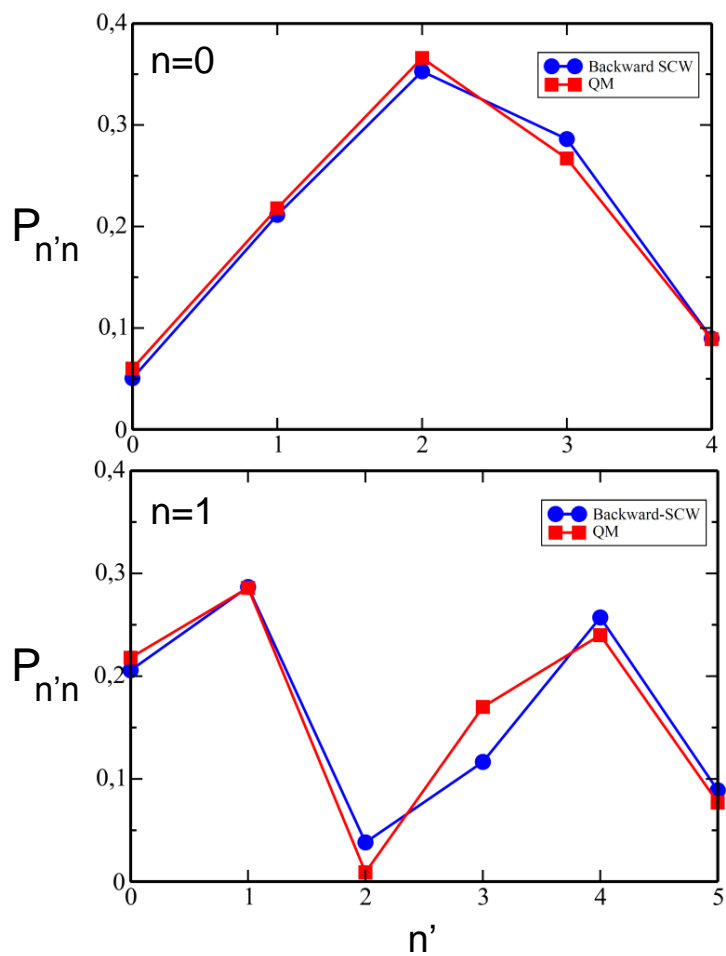


FIG. 8: Final vibrational state distribution for the Secret-Johnson model of collinear collision $\text{He}+\text{H}_2(n) \rightarrow \text{He}+\text{H}_2(n')$ at a total energy of 10. Backward-SCW predictions, given by Eq. (56), are compared with QM results.

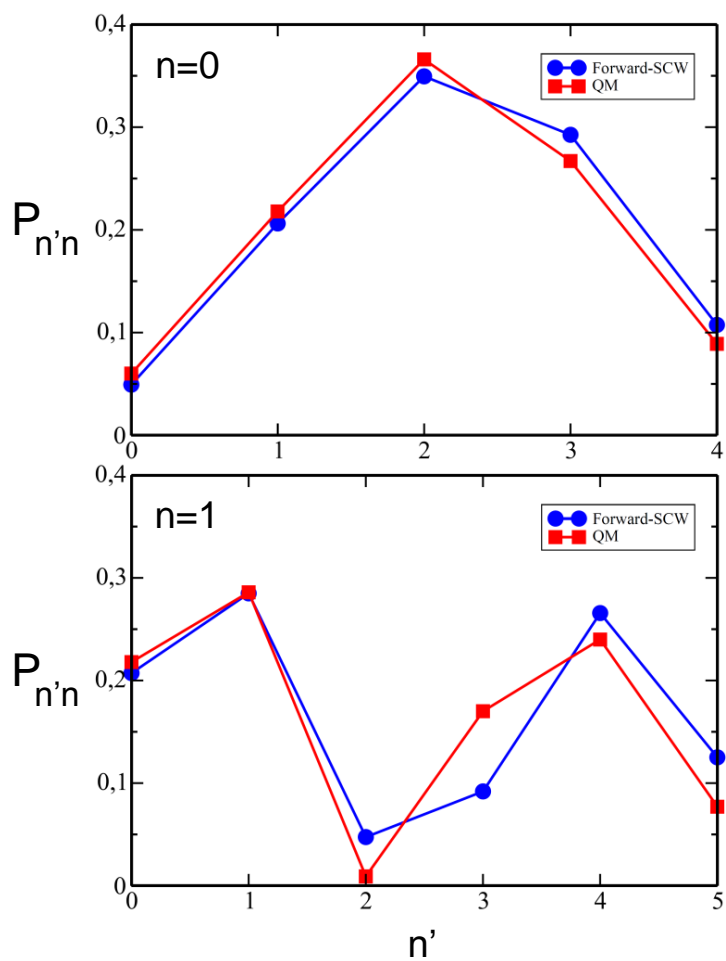


FIG. 9: Final vibrational state distribution for the Secret-Johnson model of collinear collision $\text{He}+\text{H}_2(n) \rightarrow \text{He}+\text{H}_2(n')$ at a total energy of 10. Forward-SCW predictions, given by Eq. (60), are compared with QM results.

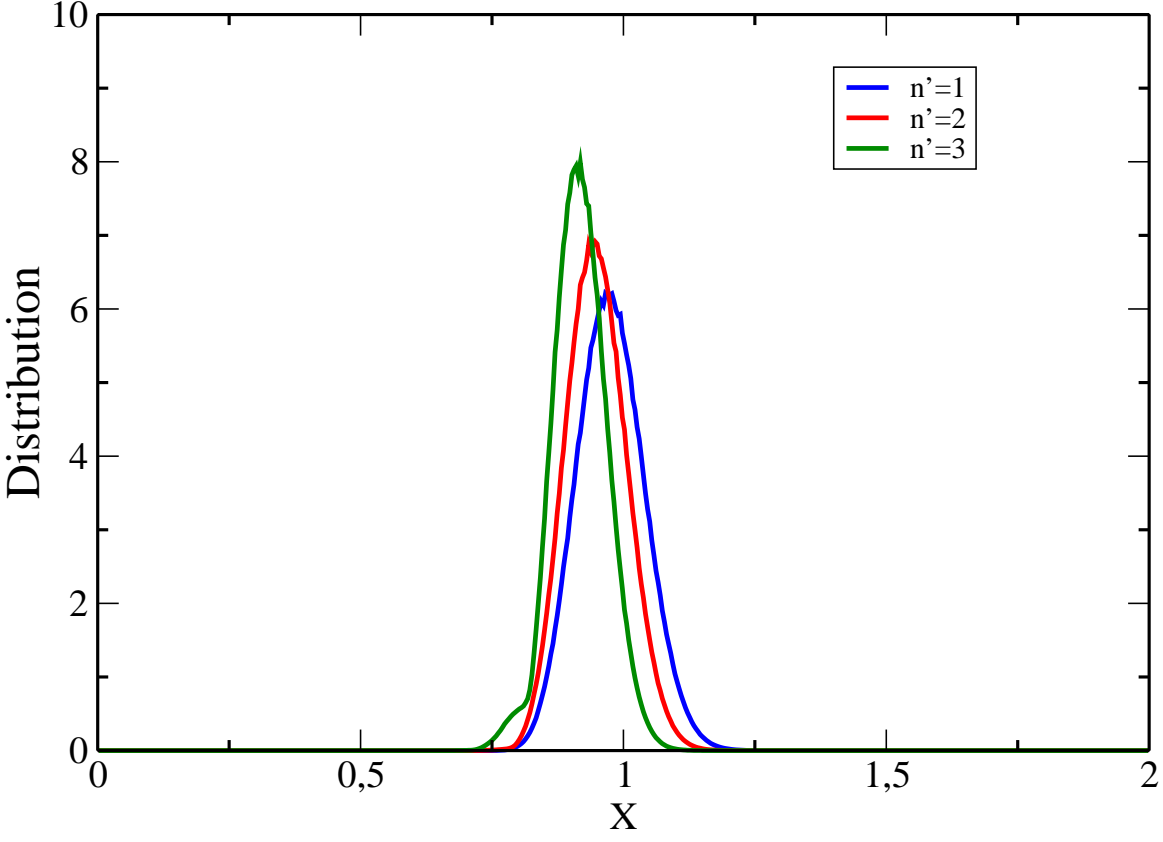


FIG. 10: Distribution of the quantity $X = \hbar k_{n'}/P_f$ for $n = 0$ and $n' = 1 - 3$.